

# Phase structure of magnetized 2SC quark matter under compact star conditions

M. Coppola<sup>1,2</sup>, P. Allen<sup>1</sup>, A.G. Grunfeld<sup>1,2</sup>, and N.N. Scoccola<sup>1,2,3</sup>

<sup>1</sup>*Department of Theoretical Physics, Comisión Nacional de Energía Atómica,  
Av. Libertador 8250, 1429 Buenos Aires, Argentina*

<sup>2</sup>*CONICET, Rivadavia 1917, 1033 Buenos Aires, Argentina*

<sup>3</sup>*Universidad Favaloro, Solís 453, 1078 Buenos Aires, Argentina*

Some properties of magnetized two flavor color superconducting (2SC) cold dense quark matter under compact star conditions (COSC) are investigated within a  $SU(2)_f$  Nambu Jona-Lasinio type model. We study the phase diagram for several model parametrizations. The features of each phase are analyzed through the behavior of the chiral and superconducting condensates for increasing chemical potential or magnetic field. We show how the phases are modified in the presence of  $\beta$ -equilibrium as well as color and electric charge neutrality conditions.

## I. INTRODUCTION

During the last years many works in the literature were devoted to the study of strongly interacting matter under the influence of strong magnetic fields (see e.g. [1] and refs. therein). In the astrophysics scenario, this is motivated by the fact that certain compact objects called magnetars can have surface magnetic fields up to  $10^{15}$  G [2], with estimates for the magnetic field values at their centers of a few orders of magnitude larger [3]. There, the relevant region of the QCD phase diagram is that of low temperature and intermediate values of density, where color superconducting (CSC) phases of quark matter are expected to exist. In this regime lattice QCD (LQCD) calculations are hindered by the well-known sign problem. Effective models of QCD arise then as a powerful tool to circumvent these problems. One of these models is the Nambu Jona-Lasinio (NJL) model [4] in which quarks are assumed to interact locally. The local character of the interactions leads to divergences in the momentum integrals that need to be regularized. When the magnetic field is introduced, the vacuum energy acquires a Landau level (LL) structure and additional care is required in the treatment of the divergences. A convenient regularization method is the so-called “Magnetic Field Independent Regularization” (MFIR) scheme [5, 6], where unphysical oscillations (that occur in other regularization schemes) are completely removed. In this contribution we present a brief report on the analysis of the behavior of magnetized 2SC quark matter under color and electric charge neutrality as well as  $\beta$ -equilibrium, which will be referred to as COSC, in the framework of NJL-type model using the MFIR scheme. Further details of this work can be found in Ref. [7].

## II. THE MODEL AND ITS REGULARIZATION

We consider a Lagrangian density composed of a quark sector, described by a NJL-type  $SU(2)_f$  Lagrangian density which includes scalar-pseudoscalar and color pairing interactions, and a leptonic contribution. In the presence of an external magnetic field and finite chemical poten-

tials it reads

$$\begin{aligned} \mathcal{L} = & \bar{\psi} \left[ i \tilde{D} - m_c + \hat{\mu} \gamma^0 \right] \psi + G \left[ (\bar{\psi} \psi)^2 + (\bar{\psi} i \gamma_5 \vec{\tau} \psi)^2 \right] \\ & + H \left[ (i \bar{\psi}^C \epsilon_f \epsilon_c^3 \gamma_5 \psi) (i \bar{\psi} \epsilon_f \epsilon_c^3 \gamma_5 \psi^C) \right] \\ & + \sum_{l=e,\mu} \bar{\psi}_l \left[ i \gamma^\mu (\partial_\mu - i e A_\mu) - m_l + \mu_l \gamma^0 \right] \psi_l. \end{aligned} \quad (1)$$

Here,  $G$  and  $H$  are coupling constants,  $\psi = (u, d)^T$  represents a quark field with two flavors,  $\psi^C = C \bar{\psi}^T$  and  $\bar{\psi}^C = \psi^T C$ , with  $C = i \gamma^2 \gamma^0$ , are charge-conjugate spinors and  $\vec{\tau} = (\tau_1, \tau_2, \tau_3)$  are Pauli matrices. Moreover,  $(\epsilon_c^3)^{ab} = (\epsilon_c)^{3ab}$  and  $(\epsilon_f)^{ij}$  are antisymmetric matrices in color and flavor space respectively. Note that we adopt the usual 2SC ansatz  $\Delta_5 = \Delta_7 = 0$ ,  $\Delta_2 = \Delta$ , where the blue quark is unpaired [4]. The (current) quark mass  $m_c$  is taken as equal for both up and down flavors, while  $m_e = 0.511$  MeV and  $m_\mu = 105.66$  MeV. The presence of an external magnetic field is introduced through the covariant derivative  $\tilde{D}_\mu = \partial_\mu - i \tilde{e} \tilde{Q} \tilde{A}_\mu$ , where  $\tilde{A}_\mu$  is a massless rotated  $U(1)$  field [8]. In units of  $\tilde{e}$  the associated rotated charges are:  $\tilde{q}_{ub} = 1$ ,  $\tilde{q}_{ur} = \tilde{q}_{ug} = 1/2$ ,  $\tilde{q}_{dr} = \tilde{q}_{dg} = -1/2$  and  $\tilde{q}_{db} = 0$ . In the present work we consider a static and constant magnetic field in the 3-direction,  $\tilde{A}_\mu = \delta_{\mu 2} x_1 B$ . In order to describe the system as a function of  $\tilde{e} B$ , we will take  $\tilde{e} = e \cos \theta \simeq e$  and  $\tilde{A}_\mu \simeq A_\mu$  as a good approximation based on the small estimated value of  $\theta$  [9].

In what follows we work in the mean field approximation (MFA), assuming that the only non-vanishing expectation values are  $\langle \bar{\psi} \psi \rangle = -(M - m_c)/2G$  and  $\langle i \bar{\psi}^C \epsilon_f \epsilon_c^3 \gamma_5 \psi \rangle = -\Delta/2H$ , which can be chosen to be real. Here,  $M$  and  $\Delta$  are the so-called dressed quark mass and superconducting gap, respectively.

The quark chemical potential is introduced through the diagonal matrix  $\hat{\mu} = (\mu_{ur}, \mu_{ug}, \mu_{ub}, \mu_{dr}, \mu_{dg}, \mu_{db}) = \mu + Q\mu_Q + T^8 \mu_8$ . Here  $\mu$  is the common chemical potential for non-zero baryonic density while  $\mu_8$  and  $\mu_Q$  are added to ensure color and electric charge neutrality conditions respectively. The six quantities  $\mu_{fc}$  are in principle independent parameters, but become related among themselves under COSC. On one hand, the quarks paired by the interaction are degenerate. Since for the chosen ansatz red and green quarks are paired, their densities

will be equal and we can impose  $\mu_3 = 0$ , which implies  $\mu_{ur} = \mu_{ug}$  and  $\mu_{dr} = \mu_{dg}$ . On the other, assuming that no neutrinos are trapped in the system,  $\beta$ -equilibrium conditions lead to  $\mu_\mu = \mu_e$  and  $\mu_{dc} = \mu_{uc} + \mu_e$ , where the latter implies  $\mu_Q = -\mu_e$ . For calculational simplicity, it is also convenient to define

$$\bar{\mu} = \frac{\mu_{dg} + \mu_{ur}}{2}, \quad \delta\mu = \frac{\mu_{dg} - \mu_{ur}}{2} = \frac{1}{2}\mu_e. \quad (2)$$

The resulting MFA thermodynamic potential at vanishing temperature reads

$$\Omega_{\text{MFA}} = \frac{(M - m_c)^2}{4G} + \frac{\Delta^2}{4H} - \sum_{|\bar{q}|=0, \frac{1}{2}, 1} P_{|\bar{q}|} - P_{lep}. \quad (3)$$

The pressures appearing in Eq. (3) read

$$P_0 = \int \frac{d^3p}{(2\pi)^3} (E_{db}^+ + |E_{db}^-|), \quad (4)$$

$$P_1 = \frac{\tilde{e}B}{8\pi^2} \sum_{k=0}^{\infty} \alpha_k \int_{-\infty}^{\infty} dp_z (E_{ub}^+ + |E_{ub}^-|), \quad (5)$$

$$P_{1/2} = \frac{\tilde{e}B}{8\pi^2} \sum_{k=0}^{\infty} \alpha_k \int_{-\infty}^{\infty} dp_z \sum_{\lambda, s=\pm} E_{\Delta^s}^\lambda, \quad (6)$$

$$P_{lep} = \sum_{l=e, \mu} P_l \Big|_{M=m_l, \mu_{ub}=\mu_l}. \quad (7)$$

Here, we have introduced  $\alpha_k = 2 - \delta_{k0}$  and

$$E_{db}^\pm = \sqrt{p^2 + M^2} \pm \mu_{db}, \quad (8)$$

$$E_{ub}^\pm = \sqrt{p_z^2 + 2k\tilde{e}B + M^2} \pm \mu_{ub}, \quad (9)$$

$$E_{\Delta^s}^\lambda = \sqrt{\left(\sqrt{p_z^2 + k\tilde{e}B + M^2} + \lambda\bar{\mu}\right)^2 + \Delta^2 + s\delta\mu}. \quad (10)$$

To regularize the divergent expressions in Eqs. (4-7) we use the MFIR scheme, where the divergence is removed by subtracting a vacuum term with the form of the  $\tilde{e}B=0$  case. The remaining magnetic field-dependent contributions turn out to be finite, and the vacuum terms are regularized with a sharp 3D cutoff [5, 6]. It is worth mentioning that when  $P_{1/2}$  is regularized, a term proportional to  $\Theta(\delta\mu - \Delta)$  appears. One can therefore distinguish between two possible situations within a  $\Delta \neq 0$  phase: a “gapless phase” ( $g2SC$ ) when  $\delta\mu > \Delta$ , and an ordinary  $2SC$  phase when  $\Delta > \delta\mu$ . The source of the differences between these phases comes from the changes in the quasi-particle spectrum in Eq. (10). As explained in Ref. [10], when  $\delta\mu \neq 0$  the gap equation has two branches of solutions and the modes are no longer completely degenerate, but they split into pairs of two with gaps  $\Delta_\pm = \Delta \pm \delta\mu$ . While in the  $2SC$  phase the four modes are gapped, in the  $g2SC$  phase the lower dispersion relation for the quasi-particle crosses the zero-energy axis and two of the four modes become gapless.

Given the regularized form of Eq. (3),  $\Omega_{\text{MFA}}^{\text{reg}}$ , the minimum for fixed values of  $\mu$  and  $\tilde{e}B$  is found by solving the

gap equations subject to the neutrality conditions

$$\frac{\partial \Omega_{\text{MFA}}^{\text{reg}}}{\partial \xi} = 0, \quad \xi = M, \Delta, \mu_8, \mu_e. \quad (11)$$

The density of each particle species is obtained by deriving the thermodynamical potential with respect to the corresponding chemical potential.

We will consider two  $SU(2)_f$  NJL model parametrizations. They are listed in Table I, where  $M_0$  represents the vacuum effective quark mass in the absence of external magnetic fields.

TABLE I. Parameter sets for the  $SU(2)_f$  NJL model. In both cases, empirical values in vacuum for the pion observables are reproduced,  $m_\pi = 138$  MeV and  $f_\pi = 92.4$  MeV.

	$M_0$ MeV	$m_c$ MeV	$G\Lambda^2$ -	$\Lambda$ MeV	$- \langle u\bar{u} \rangle^{1/3}$ MeV
Set 1	340	5.59	2.21	621	244
Set 2	400	5.83	2.44	588	241

### III. NUMERICAL RESULTS

We consider the ratio  $H/G=0.75$ , which is favored by various models of the quark effective interaction. We find the presence of  $B$ ,  $D$ , and  $A$  phases, where  $D$  and  $A$  can in turn find themselves in a  $g2SC$  or a  $2SC$  mode. Their main characteristics are summarized in Table II. Note that MC and IMC stand for “Magnetic Catalysis” [11] and “Inverse Magnetic Catalysis” [12], respectively. Meanwhile, vA-dH refers to “van Alphen-de Haas” transitions.

TABLE II. Characteristics and convention of each phase.

Phase	Characteristics
$B$ - Vacuum	$\chi$ -symmetry broken, $M = M(B, \mu=0)$ , MC, low $\mu$ , $\mu < M$ , $\Delta = \mu_8 = \mu_e = n = 0$
$A$ - CSC	$\chi$ -symmetry almost restored, IMC, big $\mu$ , $(\Delta, \mu_8, \mu_e, n) \neq 0$ , vA-dH transitions
$D$ - Mixed	$M_B > M_D > M_A$ , IMC, $(\Delta, \mu_e, n)_A > (\Delta, \mu_e, n)_D > (\Delta, \mu_e, n)_B$
-----	-----
2SC	$\Delta_\pm > \delta\mu$ , four gapped, $n_{dr} = n_{ur}$
$g2SC$ -Gapless	$\Delta_\pm < \delta\mu$ , two gapless, $n_{dr} \neq n_{ur}$
	Present in D and A. Doubly-degenerate modes with gaps $\Delta_\pm = \Delta \pm \delta\mu$

In the left panel of Fig. 1 we show the results for  $M$ ,  $\Delta$ ,  $\mu_e$  and  $\mu_8$  as a function of  $\mu$  for three representative values of  $\tilde{e}B$  within Set 1. For clarity, the different phases

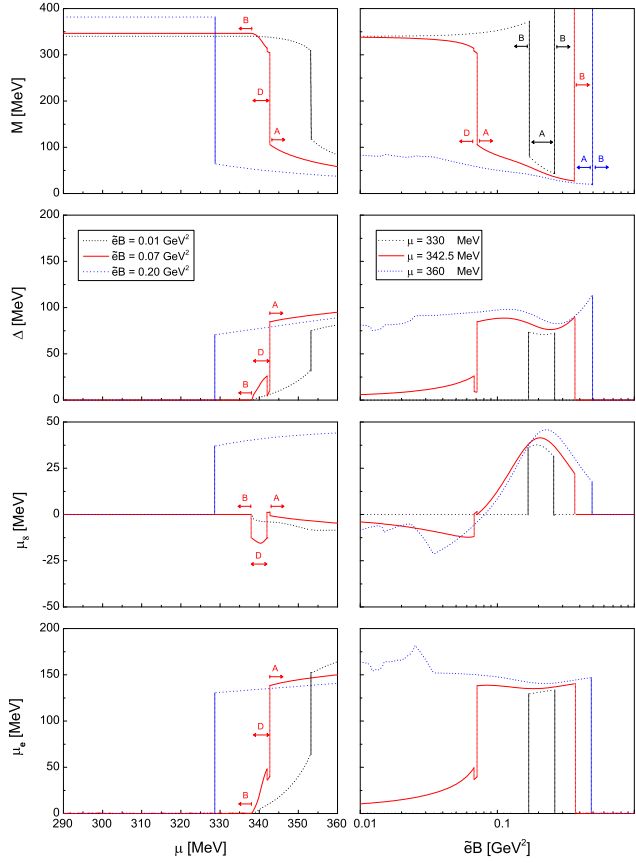


FIG. 1. (Color online)  $M$ ,  $\Delta$ ,  $\mu_8$  and  $\mu_e$  for  $H/G = 0.75$  within Set 1 considering three representative fixed values. Left: vs  $\mu$  for fixed  $\tilde{e}B$ . The A, B, D labels correspond to  $\tilde{e}B = 0.07 \text{ GeV}^2$ . Right: vs  $\tilde{e}B$  for fixed  $\mu$ .

are labeled for the  $\tilde{e}B = 0.07 \text{ GeV}^2$  case. Near the transition to the superconducting A phase,  $M$  takes values around 100 MeV and diminishes toward a value slightly above  $m_c$  for higher chemical potentials. As for  $\Delta$  and  $\mu_e$ , they increase with  $\mu$  in the range considered and can both acquire high values. In general,  $\Delta$  can reach values of the order of 100 MeV, while  $\mu_e < 200 \text{ MeV}$  and  $\mu_8$  will lie in the range  $|\mu_8| < 30 \text{ MeV}$ , varying between positive and negative values. The transition from B or D to A is of first order, while the transition from B to D is of second order. We should also note that  $\mu_8$  appears to be discontinuous along this transition. However, we bear in mind that in the B phase its value is actually not well-defined, and since it is arbitrarily taken to be zero, such discontinuity has no physical meaning.

Superconductivity is suppressed with respect to the case without COSC [6]. The presence of  $\mu_e$  separates the Fermi momenta of the up and down quarks with respect to each other. Since the quark pairing occurs between particles of equal and opposite momenta, this splitting reduces the diquark condensate. It can be interpreted that, due to this suppression, the D phase exists because the A phase with larger  $\Delta$  is energetically disfavored with

respect to the former.

For  $\tilde{e}B = 0.07 \text{ GeV}^2$ , we see that immediately after the second order transition from B to D,  $\Delta \gtrsim \delta\mu$ , so the system is in the 2SC mode. However, these two quantities are very similar, and when the chemical potential is increased  $\delta\mu$  becomes larger than  $\Delta$  for  $\mu \simeq 342 \text{ MeV}$ , leading to a  $g2SC$  region.

We turn now to the right panel of Fig. 1. We find that, in the B phase,  $M$  always increases with the magnetic field according to the MC effect, which occurs principally in vacuum. Particularly, this can be seen in the figure for the  $\mu = 330 \text{ MeV}$  case. In the D phase,  $M$  decreases slowly with  $\tilde{e}B$ , exhibiting the behavior of IMC. In the A phase we see a series of near vertical first order transitions. They are related to the vA-dH effect and their origin lies in the quantization in LL's of the dispersion relations of quarks and leptons under the influence of magnetic fields, according to Eq. (9). An important point is that no oscillations of the parameters are present in the B phase, in contrast to previous studies which use smooth regularization functions [13, 14]. This is because the MFIR scheme removes these strong unphysical oscillations, also assuring that all of the oscillations present in the A phase are real vA-dH transitions.

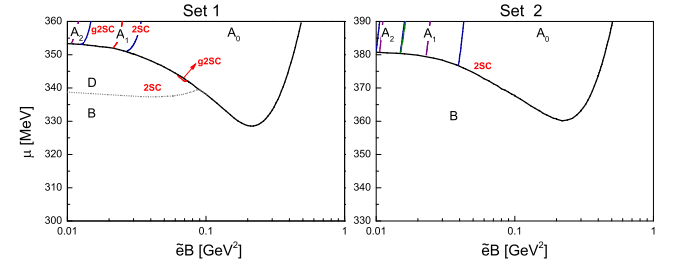


FIG. 2. (Color online) Phase diagrams for  $H/G = 0.75$ , for both Set 1 (left) and Set 2 (right). Full lines correspond to first order transitions and dotted lines to second order transitions. Black lines represent phase transitions. VA-dH transitions for unit charged species are colored as: blue for  $ub$  quarks, violet for electrons and green for muons. Red lines indicate  $g2SC$ - $2SC$  transitions.

The corresponding phase diagrams in the  $\tilde{e}B - \mu$  plane are given in Fig. 2 for the two parameter sets considered. Since Set 2 corresponds to a higher value of  $M_0$  the transitions are displaced to higher chemical potentials. For Set 2 only phases B and A exist. In Set 1, instead, phases B, D and A are present, where the latter two can exist both in the  $g2SC$  or the 2SC modes. We will concentrate on Set 1 in what follows. The behavior as a function of  $\tilde{e}B$  of the first order transition leading to the A-type phases is worth noting: for small fields, the transition has a small downward slope, which becomes sharper as the magnetic field is increased, forming a well-shaped curve. This effect is related to the so-called IMC effect [12]. From comparison with [6], COSC tend to decrease the IMC effect: the depth of the well decreases.

The B phase is present for low chemical potentials

( $\mu \lesssim 330$  MeV). Moreover, in the MFIR scheme it is always recovered for high enough magnetic fields. Regarding the  $D$  phase, its presence depends on the set of parameters. The existence of this intermediate mixed phase is a consequence of the diquark pairing alone and hence is already present for zero magnetic field, extending itself in the horizontal direction.

In the  $A$  phase we see the presence of the already mentioned vA-dH transitions. They are similar to those discussed in [6]. However, in the 2SC case with a rotated magnetic field under COSC only the  $ub$  quarks and leptons exhibit ordinary vA-dH transitions as in the basic NJL model. The  $db$  quarks are not coupled to the field, so the form of the dispersion relation is that of the free quark. As for the paired  $r$  and  $g$  quarks, all of their LL's are usually populated when  $\Delta \neq 0$ . Only in the g2SC phase the  $P_{1/2}$  term may contain a sum over LL's which is cut off by a Heaviside function. However, the origin of this transitions is different from that of the vA-dH ones. The effect of these transitions is smeared out as  $H/G$  is increased. Since they are numerous and become rather weak to affect the order parameters in a visible way, we have not included them in the phase diagram. In the  $A_i$  sub-phases of Fig. 2, the  $ub$  quark populates up to the  $i$ -th LL. If we traverse the phase diagram horizontally in the increasing  $\vec{e}B$  direction, the highest populated LL of a particular unit charged species decreases in one unit every time one of the corresponding transitions is crossed. In the  $A_0$  phase, both  $ub$  quarks and leptons are in the LLL. The maximum LL populated in these phase diagrams is smaller than the one obtained in: (a) the symmetric matter case, because  $\mu_e$  reduces  $\mu_{ub}$ , and (b) the model without superconductivity, because  $\tilde{q}_{ub} > q_u, |q_d|$ . Note that for  $H/G = 0.75$ , in the  $D$  phase there is a small gapless region, bounded by first order transitions. From analyzing the  $B = 0$  case, this region is expected to grow rapidly when  $H/G$  is decreased between 0.75 and 0.7.

Although the ratio  $H/G = 0.75$  is favored by various models of the quark effective interaction, from a more phenomenological point of view this value is subject to rather large uncertainties. For this reason, another rep-

resentative value of this ratio,  $H/G = 1$ , was considered in [7]. In that case, superconducting effects are enhanced and  $\Delta$  can reach values of the order of 200 MeV. This will induce an increase in the density of paired quarks. To maintain color neutrality,  $\mu_s$  is lowered, lying in the range  $|\mu_s| < 70$  MeV, while  $\mu_e$  is only slightly modified.

#### IV. CONCLUSIONS

As expected, several effects take place on the behavior of the cold magnetized 2SC quark matter when introducing COSC. Their presence induces the existence of  $g2SC$  and  $2SC$  modes, and reduces the maximum Landau level reached in the vA-dH transitions. In general, charge neutrality constraints tend to reduce the superconducting effect, increasing the value of the critical chemical potentials and attenuating the magnetic catalysis effect, diminishing the depth of the IMC well. As a consequence, the phase diagram is moved to higher ranges of  $\mu$  favoring different phases. In this work we analyzed the usual  $H/G = 0.75$  ratio. For higher ratios superconducting effects are enhanced:  $\Delta$  is increased, the phase diagram is brought to lower ranges of  $\mu$  and the IMC well widens and shortens [7]. For values of  $H/G \gtrsim 1$  (which are unlikely to be realized in QCD) the structure of the phase diagram is expected to be maintained, with the difference that the first order transition between the  $D$  and  $A$  phases weakens and eventually turns into a crossover around  $H/G \sim 1.15$ . In particular, for  $H/G < 0.65$  it is expected that the superconducting gap vanishes in the  $C$  and  $A$  phases.

#### ACKNOWLEDGEMENTS

This work has been funded in part by CONICET (Argentina) under Grant No. PIP 578 and by ANPCyT (Argentina) under Grant No. PICT-2014-0492.

- 
- [1] J. O. Andersen, W. R. Naylor and A. Tranberg, Rev. Mod. Phys. **88**, 025001 (2016); V. A. Miransky and I. A. Shovkovy, Phys. Rept. **576**, 1 (2015)
  - [2] R. C. Duncan and C. Thompson, Astrophys. J. **392**, L9 (1992); B. Paczynski, Acta Astron., **42**, 145 (1992)
  - [3] D. Chatterjee et al., Mon. Not. Roy. Astron. Soc. **447**, 3785 (2015); D. Lai and S. L. Shapiro, Astrophys. J. **383**, 745 (1991); D. Bandyopadhyay, S. Chakrabarty and S. Pal, Phys. Rev. Lett. **79**, 2176 (1997); E. J. Ferrer et al., Phys. Rev. C **82**, 065802 (2010)
  - [4] U. Vogl and W. Weise, Prog. Part. Nucl. Phys. **27**, 195 (1991); S. Klevansky, Rev. Mod. Phys. **64**, 649 (1992); T. Hatsuda and T. Kunihiro, Phys. Rep. **247**, 221 (1994); M. Buballa, Phys. Rept. **407**, 205 (2005)
  - [5] D. P. Menezes et al., Phys. Rev. C **79**, 035807 (2009)
  - [6] P. G. Allen, A. G. Grunfeld and N. N. Scoccola, Phys. Rev. D **92**, 074041 (2015)
  - [7] M. Coppola et al., Phys. Rev. D **96** 056013 (2017)
  - [8] M. G. Alford, J. Berges and K. Rajagopal, Nucl. Phys. B **571**, 269 (2000)
  - [9] E. V. Gorbar, Phys. Rev. D **62**, 014007 (2000)
  - [10] M. Huang and I. Shovkovy, Nucl. Phys. A **729**, 835 (2003); I. A. Shovkovy, Found. Phys. **35**, 1309 (2005)
  - [11] I. A. Shovkovy, Lect. Notes Phys. **871**, 13 (2013)
  - [12] F. Preis, A. Rebhan and A. Schmitt, Lect. Notes Phys. **871**, 51 (2013)
  - [13] S. Fayazbakhsh and N. Sadooghi, Phys. Rev. D **82**, 045010 (2010)
  - [14] T. Mandal and P. Jaikumar, Phys. Rev. C **87**, 045208 (2013)